

Local-moment formation and metal–nonmetal transition in $\text{Ca}_{1-x}\text{Y}_x\text{VO}_3$ and $\text{Ca}_{1-x}\text{Y}_x\text{TiO}_3$

Y NISHIHARA^{1,*}, H KAWANAKA² and H BANDO²

¹Faculty of Science, Ibaraki University, Mito, Ibaraki 310-8512, Japan

²National Institute of Advanced Industrial Science and Technology, Tsukuba, Ibaraki 305-8568, Japan

*Email: ynishi@mito.ipc.ibaraki.ac.jp

Abstract. Electron-doped metallic states of $\text{Ca}_{1-x}\text{Y}_x\text{VO}_3$ and $\text{Ca}_{1-x}\text{Y}_x\text{TiO}_3$ change into non-metallic states around $x \sim 0.4$ and 0.6 , respectively. The residual resistivity in the metallic states increases with increasing effective magnetic moment or coefficient of T^2 term of resistivity. The effective moment reaches $\sim 0.5 \mu_B/\text{molecule}$ in $\text{Ca}_{1-x}\text{Y}_x\text{VO}_3$ and also in $\text{Ca}_{1-x}\text{Y}_x\text{TiO}_3$ near the metal–nonmetal phase boundary. In these metallic states, $\sim 10\%$ of $3d$ atoms seem to have large localized magnetic moments. In electron-doped metallic sample of $\text{Ca}_{1-x}\text{Y}_x\text{VO}_3$, the temperature dependence of resistance shows no resistance-minimum. However, weak negative magneto-resistance is observed for the sample with $x = 0.2$ up to 50 Tesla at 4.2 K.

Keywords. Metal–nonmetal phase boundary; local moment formation; $\text{Ca}_{1-x}\text{Y}_x\text{VO}_3$.

PACS Nos 75.20.Hm; 71.30.+h

1. Introduction

The perovskite-type compounds $\text{Ca}_{1-x}\text{Y}_x\text{VO}_3$ and $\text{Ca}_{1-x}\text{Y}_x\text{TiO}_3$ have been intensively studied as typical filling-control metal–insulator transition systems [1–5]. However, in most real materials electronic interaction coexists with randomness. In strongly correlated electron systems the randomness easily induces local magnetic moments. It is expected that this local moment formation has a strong influence on the metal–insulator transition. The study of interaction between electrons and disorder is one of the most interesting problems in correlation between magnetism and transport phenomena [6,7].

CaVO_3 is a metal with one $3d$ electron and CaTiO_3 an insulator without $3d$ electrons. With increasing d electron numbers x , CaTiO_3 shows metallic conductivity. The metallic states of CaVO_3 and CaTiO_3 change into nonmetallic states around $x \sim 0.4$ and 0.6 , respectively. In both systems doped electrons induce local magnetic moments and the temperature dependence of magnetic susceptibility changes from the Pauli paramagnetic type to the Curie–Weiss type with increasing d electrons. From the analysis of magnetic susceptibility $\sim 10\%$ of $3d$ atoms seem to have large localized magnetic moments in these metallic states. Formation of local magnetic moment is closely related with the increase in resistivity and at low temperatures negative magneto-resistance is observed. In this paper

experimental results and discussion about correlation between magnetism and transport properties are reported.

2. Experimental results in $\text{Ca}_{1-x}\text{Y}_x\text{VO}_3$

Samples of $\text{Ca}_{1-x}\text{Y}_x\text{VO}_3$ were prepared by floating zone method using xenon lamp image furnace. The crystals were grown at the rate of 10 to 20 mm/s in high purity Ar gas. The oxygen content of the samples with $x > 0.2$ is nearly stoichiometric. The samples with $x < 0.2$ were oxygen deficient and stoichiometric samples were obtained by annealing at 500°C in air. The temperature dependence of resistivity changes with Y concentration as shown in figure 1. The samples with $x < 0.4$ show metallic behavior in the temperature regions investigated, and those with $x \geq 0.6$ show activation type semi-conductive behavior. The activation energy is ~ 0.2 eV for the sample with $x = 0.7$. The resistivity in the metallic region is proportional to the square of the temperature. The elastic electron-impurity scattering seems to be a dominant scattering mechanism in these metallic states [8]. The samples with x between 0.4 and 0.6 are metallic in the high temperature region. However, the resistivity increases with decreasing temperature at low temperatures and approaches finite values at $T = 0$ in contrast with that of samples with $x > 0.6$.

The magnetic susceptibility of the metallic sample is expressed by a summation of the temperature independent χ_0 term and the temperature dependent Curie-Weiss term. The temperature dependence of magnetic susceptibility for $0.4 < x < 0.7$ shows a peak at around 25 K. The peak is continuously connected with the anti-ferromagnetic transition

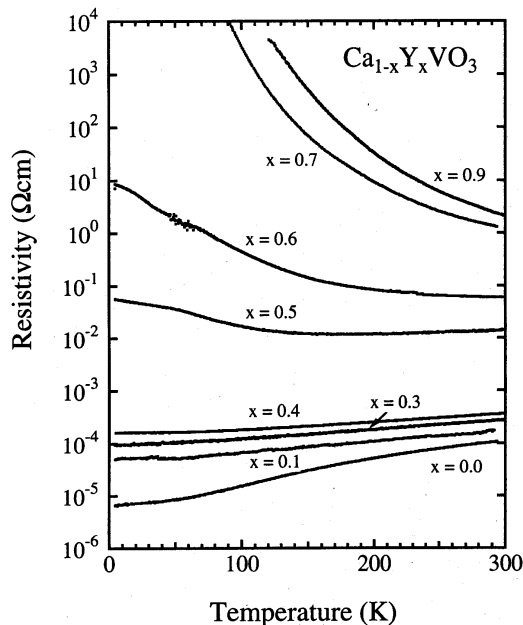


Figure 1. Temperature dependence of the resistivity in $\text{Ca}_{1-x}\text{Y}_x\text{VO}_3$.

temperature of YVO_3 . Figure 2 shows the Y concentration dependence of χ_0 value and the effective magnetic moment μ_{eff} /molecule estimated from the Curie–Weiss term. The values of χ_0 and μ_{eff} gradually increase with increasing Y concentration up to $x \sim 0.4$. The χ_0 shows a peak at $x \sim 0.4$ and the μ_{eff} values start to rapidly increase above $x \sim 0.4$, where the semi-conductive behavior of the resistivity appears. The effective magnetic moment increases with d electrons and reaches $\sim 0.5 \mu_B$ /molecule in $\text{Ca}_{1-x}\text{Y}_x\text{VO}_3$ and, also, in $\text{Ca}_{1-x}\text{Y}_x\text{TiO}_3$ [9,10] near the metal–nonmetal phase boundary.

We measured the magneto-resistance at 4.2 K. The well-annealed CaVO_3 shows a positive magneto-resistance. This positive magneto-resistance is proportional to the square of the magnetic field and does not saturate up to 12 Tesla [11]. However, this positive magneto-resistance rapidly decreases with substitution of Ca by Y or the introduction of oxygen vacancy. The value of positive magneto-resistance, $\delta\rho/\rho \sim 120\%$ at 10 Tesla, becomes nearly zero for Y concentration of $x = 0.1$, and it becomes negative for $x = 0.2$, as shown in the figure 3. The negative magneto-resistance of $x = 0.2$ stays up to 50 Tesla. In general, the magneto-resistance is expressed as a sum of the negative and positive components, as observed in the dilute magnetic alloys. However, in this system the positive component does not seem to be present. Much larger negative magneto-resistance is observed in the CaVO_3 with oxygen vacancy [11,12]. The value of the magneto-resistance, $\delta\rho/\rho$ reaches -12.5% at 5 Tesla for $\text{CaVO}_{2.8}$ [12]. In contrast to the Kondo alloys, the temperature dependence of resistivity shows no resistance-minimum in these systems.

3. Discussion

3.1 Phase diagrams of $\text{Ca}_{1-x}\text{Y}_x\text{VO}_3$ and $\text{Ca}_{1-x}\text{Y}_x\text{TiO}_3$

In these systems, it is well-known that the electron correlation increases with increasing d electron number and the systems change from a metal to a magnetic insulator. But pre-

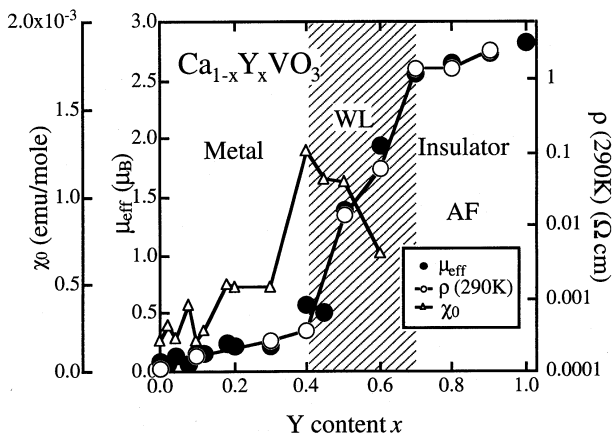


Figure 2. Y concentration dependence of the effective magnetic moment (μ_{eff}) and χ_0 . The resistivity (ρ) at the room temperature is also plotted.

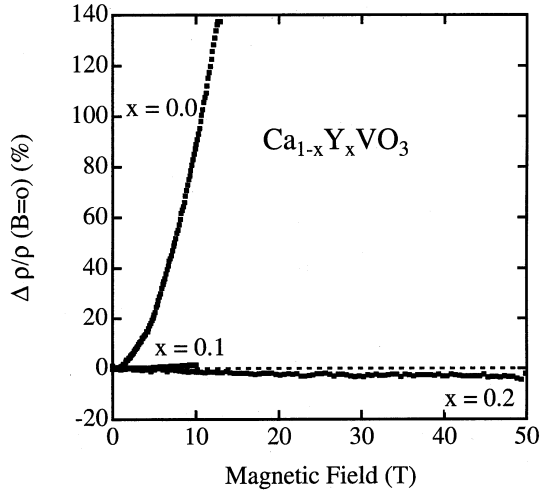


Figure 3. Magnetic field dependence of the magneto-resistance for $x = 0.1$ and 0.2 .

cise phase diagrams have not been presented yet. Figure 4 shows the phase diagrams of $\text{Ca}_{1-x}\text{Y}_x\text{VO}_3$ and $\text{Ca}_{1-x}\text{Y}_x\text{TiO}_3$. In $\text{Ca}_{1-x}\text{Y}_x\text{VO}_3$, below $x \sim 0.4$, the resistivity is expressed as a sum of the residual resistivity and the T^2 term. Between $x \sim 0.4$ and 0.6 , the resistivity shows a metallic behavior at high temperatures and increases with decreasing temperature at low temperatures. The low temperature value of the resistivity remains finite, so that we denote this region as a weak localization (WL) region and distinguish it from the activation type insulator region ($x > 0.6$). In this Y concentration region, the magnetic susceptibility exhibits a peak around 25 K. The temperature of this susceptibility peak starts to increase rapidly around the phase boundary between the WL and the insulator regions.

In $\text{Ca}_{1-x}\text{Y}_x\text{TiO}_3$, since the d electron number is less than 1, a magnetic order seems to be hard to develop compared to that in the $\text{Ca}_{1-x}\text{Y}_x\text{VO}_3$ system. The magnetic order cannot be observed below $x \sim 0.9$. The metallic state remains up to $x \sim 0.6$, and above $x \sim 0.6$, a large spin to a small spin transition appears along with a resistive-transition from semi-conductive to the metallic state. The difference in the development of magnetic order might be one of the causes for the differences that exist in these two phase diagrams.

3.2 Metal–nonmetal transition and the local moment formation

T^2 -dependent resistivity is observed in the metallic states of both $\text{Ca}_{1-x}\text{Y}_x\text{VO}_3$ and $\text{Ca}_{1-x}\text{Y}_x\text{TiO}_3$. The proportionality of the T^2 contribution to the residual resistance results from the electron-phonon-impurity interference in disordered metals [8]. From this relation we find that these systems are disordered correlated electron systems. As we approach the metal–nonmetal boundary, both disordering and the electron correlations increase and induce local magnetic moments. From the Curie–Weiss contribution in the magnetic susceptibility, we can estimate the number of magnetic V atoms. 5–10% of the V atoms are

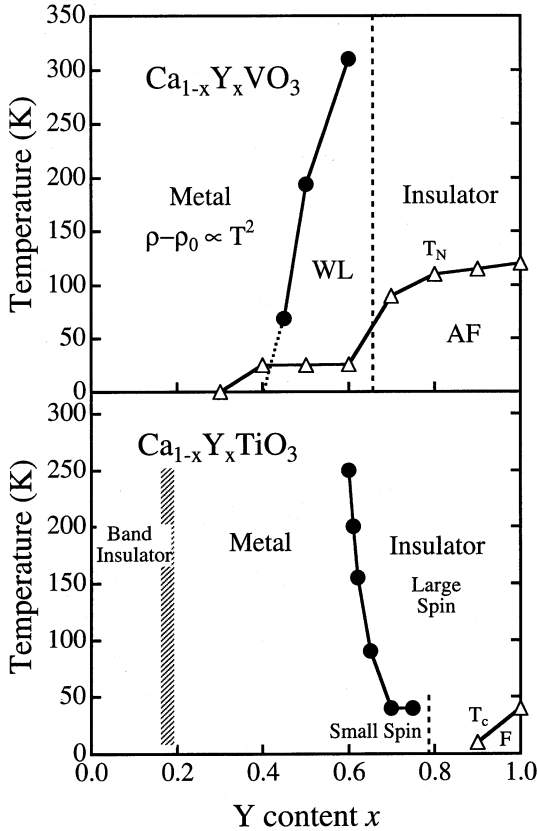


Figure 4. Phase diagrams of the $\text{Ca}_{1-x}\text{Y}_x\text{VO}_3$ and the $\text{Ca}_{1-x}\text{Y}_x\text{TiO}_3$.

magnetic around $x = 0.6$. We can take the value of effective moment as a measure of the contribution of magnetic V atoms. The Y concentration dependence of the effective magnetic moment has a strong correlation with the change in the resistance, as shown in figure 2. Both resistivity and the effective moment rapidly increase in the WL region. It is clear that the formation of the magnetic V atoms plays an essential role in the metal–nonmetal transition in this system. The same situation is observed in the $\text{Ca}_{1-x}\text{Y}_x\text{TiO}_3$. The resistivity increases with increasing effective magnetic moment in the small spin state [9,10]. The transition between the large spin to a small spin may be explained by a competition between the Mott–Hubbard phase and the Kondo effect [1,14].

4. Conclusions

In the filling-controlled metal–insulator transition systems studied in this work, we have observed that disorder induced local moments appear in the metallic state near the phase boundary. The increase in the local moments is strongly correlated with the increase in

resistivity. Our results suggest that the role of local moments should also be taken into account in the analysis of metal–insulator transition in these systems.

References

- [1] M Kasuya, Y Tokura, T Arima, H Eisaki and S Uchida, *Phys. Rev.* **B47**, 6197 (1993)
- [2] Y Taguchi, Y Tokura, T Arima and F Inaba, *Phys. Rev.* **B48**, 511 (1993)
- [3] Y Tokura, Y Taguchi, Y Moritomo, K Kumagai, T Suzuki and Y Iye, *Phys. Rev.* **B48**, 14063 (1993)
- [4] K Kumagai, T Suzuki, Y Taguchi, Y Okada, Y Fujishima and Y Tokura, *Phys. Rev.* **B48**, 7636 (1993)
- [5] H F Pen, M Abbate, A Fujimori, Y Tokura, H Eisaki, S Uchida and G A Sawatzky, *Phys. Rev.* **B59**, 7422 (1999)
- [6] M Milovanovic, S Sachder and R N Bhatt, *Phys. Rev. Lett.* **63**, 82 (1989)
- [7] V Dobrosavljevic and G Kotliar, *Phys. Rev.* **B50**, 1430 (1994)
- [8] N G Ptitsina, G M Chulkova, K S Il'in, A V Sergeev, F S Pochinkov, E M Gershenson and M E Gershenson, *Phys. Rev.* **B56**, 10089 (1997)
- [9] F Iga, T Nishiguchi and Y Nishihara, *Physica* **B206&207**, 859 (1995)
- [10] T Naka, T Matsumoto, A Matsushita, F Iga and Y Nishihara, *Physica* **B304**, 27 (2001)
- [11] A Fukushima, F Iga, I H Inoue, K Murata and Y Nishihara, *J. Phys. Soc. Jpn.* **63**, 409 (1994)
- [12] N Sirakawa, K Murata, H Makino, F Iga and Y Nishihara, *J. Phys. Soc. Jpn.* **64**, 4824 (1995)
- [13] T Pruschke, D L Cox and M Jarrell, *Phys. Rev.* **B47**, 3553 (1993)
- [14] F Iga, Y Nishihara, J Sakurai and M Ishikawa, *Physica* **B237&238**, 14 (1997)